AD-A057 065 NORTHWESTERN UNIV EVANSTON ILL DEPT OF MECHANICAL E--ETC F/G 4/1
TEST PARTICLE CORRELATION BY A WHISTLER WAVE IN A NONUNIFORM MA--ETC(U)
JUN 77 J L VOMVORIDIS, J DENAVIT N00014-75-C-0473

UNCLASSIFIED TR-8 NL

| OF |
AD
AD57065

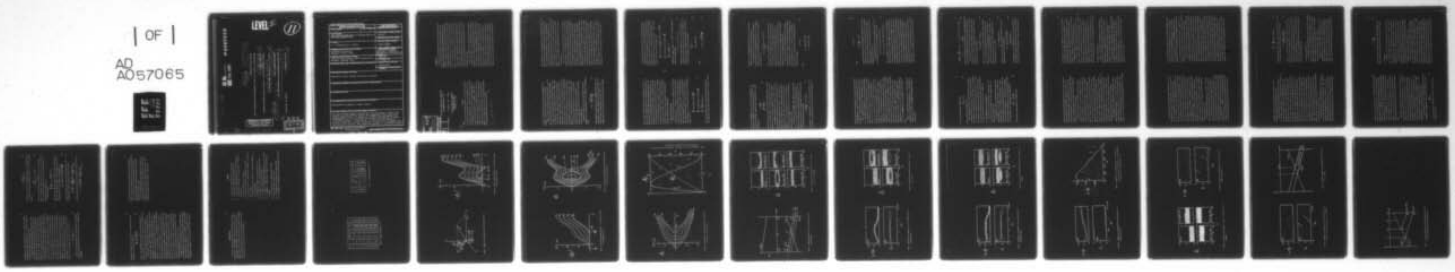

END
DATE
FILMED
9-78
DDC

(11)

(9) Technical Report No. 8

Project No. NR 012-315

(6) TEST PARTICLE CORRELATION BY A WHISTLER WAVE IN A NONUNIFORM MAGNETIC FIELD.

(14) TR-8

(10) Authors: J. L. Vomvoridis and J. Denavit

Research supported by the U. S. Office of Naval Research Contract No. (15) N00014-75-0473

(11) Jun 77 (12) 26 p.

403 502

SECURITY CLASSIFICATION OF THIS PAGE (When Data Entered)

REPORT DOCUMENTATION PAGE		READ INSTRUCTIONS BEFORE COMPLETING FORM
1. REPORT NUMBER 8	2. GOVT ACCESSION NO.	3. RECIPIENT'S CATALOG NUMBER
4. TITLE (and Subtitle) TEST PARTICLE CORRELATION BY A WHISTLER WAVE IN A NONUNIFORM MAGNETIC FIELD		5. TYPE OF REPORT & PERIOD COVERED Technical 6. PERFORMING ORG. REPORT NUMBER
7. AUTHOR(s) J. L. Vomvoridis and J. Denavit		8. CONTRACT OR GRANT NUMBER(s) N00014-75-0473
9. PERFORMING ORGANIZATION NAME AND ADDRESS Northwestern University Evanston, Illinois 60201		10. PROGRAM ELEMENT, PROJECT, TASK AREA & WORK UNIT NUMBERS Department of Mechanical Engineering and Astronautical Sciences
11. CONTROLLING OFFICE NAME AND ADDRESS Office of Naval Research, Physics Program Office Arlington, Virginia 22217		12. REPORT DATE June 1977 13. NUMBER OF PAGES 35
14. MONITORING AGENCY NAME & ADDRESS(if different from Controlling Office)		15. SECURITY CLASS. (of this report) Unclassified 15a. DECLASSIFICATION/DOWNGRADING SCHEDULE

16. DISTRIBUTION STATEMENT (of this Report)

Approved for public release; distribution unlimited.

17. DISTRIBUTION STATEMENT (of the abstract entered in Block 20, if different from Report)

18. SUPPLEMENTARY NOTES

19. KEY WORDS (Continue on reverse side if necessary and identify by block number)

Magnetospheric propagation, plasma, whistler.

20. ABSTRACT (Continue on reverse side if necessary and identify by block number)

This paper presents computer simulations of the correlation in phase of test electrons in a monochromatic whistler wave propagating along a non-uniform external magnetic field. The behavior of resonant electrons depends on an inhomogeneity ratio R, which defines the external field gradient in relation to the wave amplitude. In the case $|R| < 1$, where electron trapping is possible, a hole (or an island) of particles is found to occur in phase plots of the distribution function. This causes the appearance of a transverse current

DD FORM 1 JAN 73 1473 EDITION OF 1 NOV 65 IS OBSOLETE
S/N 0102-LF-014-6601

SECURITY CLASSIFICATION OF THIS PAGE (When Data Entered)

TEST PARTICLE CORRELATION BY A WHISTLER WAVE IN A NONUNIFORM MAGNETIC FIELD

J. L. Vomvoridis and J. Denavit

Department of Mechanical Engineering
and Astronautical Sciences
Northwestern University
Evanston, Ill. 60201

ABSTRACT

This paper presents computer simulations of the correlation in phase of test electrons in a monochromatic whistler wave propagating along a non-uniform external magnetic field. The behavior of resonant electrons depends on an inhomogeneity ratio R, which defines the external field gradient in relation to the wave amplitude. In the case $|R| < 1$, where electron trapping is possible, a hole (or an island) of particles is found to occur in phase plots of the distribution function. This causes the appearance of a transverse current coherent with the wave, which is most intense for $|R| \simeq 0.6$. The significance of these results to magnetospheric propagation of a quasi-monochromatic whistler pulse is discussed.

abs. val. R approx. = or <

I. INTRODUCTION

Earlier analytical and computer simulation studies have demonstrated the effect of trapped resonant electrons on the nonlinear evolution of large-amplitude electrostatic and whistler wavepackets propagating in uniform plasmas[1,2]. Resonant electrons with velocities near v_r travelling through a wavepacket propagating at the group velocity v_g remain in transit through the wavepacket during a time $T = \ell/|v_r - v_g|$, where ℓ denotes the wavepacket length. If the transit time T is of the same order as (or larger than) the period τ_t of trapping oscillations of electrons in the wave fields, resonant electrons become correlated relative to the wave. Such electrons then act as coherent charge or current sources causing emission of new waves, which result in distortion and elongation of the original wavepacket. In the case of electrostatic wavepackets this theory has recently been given a direct experimental verification[3].

Interaction of resonant electrons with whistler waves occurs naturally in the Earth's magnetosphere. Of particular importance is the interaction responsible for the artificially triggered discrete emissions[4,5], because of their potential use in monitoring the magnetospheric conditions (density and energy distribution of the magnetospheric electron population). A large number of theoretical investigations have been presented[6], aiming at the interpretation of these emissions. It is generally accepted that the emissions are the result of resonant or trapped particle effects, but no theory presently answers all questions satisfactorily. The appearance of emissions at frequencies different from the frequency of the triggering signal, and satellite observations of emissions not originating from the

vicinity of the equatorial plane[7], indicate that the inhomogeneity of the geomagnetic field must play an important role in these emissions.

Resonant electrons in a whistler wave have velocities near $v_r = (\omega - \Omega)/k$, where ω and k are, respectively, the wave frequency and the wave number, $\Omega = eB_o/mc$ is the electron gyrofrequency of the external field $\underset{\sim}{B}_o$, $-e$ and m are, respectively, the electron charge and mass and c is the speed of light. In the linear regime, resonant electron interactions are responsible for frequency shifts and amplitude damping or growth of the wave[8], similar to Landau damping of Langmuir waves. The linear solutions cease to be valid for times $t \geq \omega_t^{-1}$, where $\omega_t = (kv_\perp\Omega_\perp)^{1/2}$ is the small-amplitude trapping frequency of resonant electrons in the wave fields, $\underset{\sim}{v}_\perp$ is the electron velocity component perpendicular to the external field, $\Omega_\perp = eB_\perp/mc$, and $\underset{\sim}{B}_\perp$ is the wave magnetic field. Analytical and numerical studies of the nonlinear regime in a uniform external field[9,10] show that for $t > \omega_t^{-1}$ the wave amplitude oscillates near the trapping frequency and settles asymptotically to a quasi-static ergodic state. This result is also similar to the nonlinear evolution of Langmuir waves.

The dynamics of resonant electrons in a monochromatic whistler wave propagating in a non-uniform medium may be shown to depend on the inhomogeneity ratio[11]

$$R = \left(3v_r - \frac{v_\perp^2 - Kv_r^2}{\Omega/k}\right)\frac{d\Omega/dz}{2\omega_t^2} \quad , \qquad (1)$$

characterizing the relative strength of the inhomogeneity and the wave. Here, the coordinate z is measured along $\underset{\sim}{B}_o$ and an electron density proportional to Ω^K has been assumed. Trapped particles exist only for $|R| < 1$. This dynamical problem, and the similar problem of electron resonance in Langmuir

waves propagating in a non-uniform medium, have been considered by Karpman et al.[12]. These authors have derived nonlinear damping rates for the cases $|R| > 1$ and $|R| \ll 1$, based on energy conservation. For $|R| > 1$ (strong inhomogeneity), no trapped particles exist and the effect of the inhomogeneity is to continually replenish the resonance region with fresh particles, thereby maintaining quasi-Landau damping for times $t > \omega_t^{-1}$. For $|R| \ll 1$ the inhomogeneity of the medium is sufficiently weak to be considered as a perturbation. The trapped particles in this case absorb a net amount of energy from the wave and cause a nonlinear damping.

The purpose of the present paper is to present the results of detailed computer simulations of the correlation in phase of test electrons moving in a monochromatic whistler wave propagating along a non-uniform magnetic field. An analysis of resonant electron trajectories based on an invariant applicable to uniform gradients is presented in Sec. II to define the basic concepts and notations, and to enable the interpretation of the numerical results. The evolution of a test distribution under the action of a monochromatic whistler wave propagating along a magnetic field having a uniform gradient is examined numerically in Sec. III. The algorithm used[13] is based on the exact set of equations of motion and the analysis of Sec. II is used for comparison and interpretation purposes only. Since the interpretation of the emissions involves the transverse current of resonant electrons, the distribution function is Fourier analyzed to give the evolution of the first-order phase correlation (or phase bunching) of resonant electrons with respect to the wave magnetic field. Values of R ranging from $R = 0.05$ to $R = 2.5$ have been considered, including values $R \lesssim 1$ near the trapping transition. The phase plots presented in Sec. III show that for $|R| < 1$ the average trapped

electron parallel velocities remain close to the resonant velocity of the wave, v_r, while untrapped electrons move with average parallel velocities, $v_\parallel$, maintaining their energy and magnetic moment approximately constant. This results in a clear separation between trapped and untrapped electrons producing either a hole or an island of particles in the trapped region, which causes strong phase bunching of the distribution function. For values of $R > 1$, for which particle trapping is not possible, only phase correlations associated with steep gradients of the distribution function with respect to parallel velocity are found. Finally, Sec. IV discusses the significance of particle correlation to the growth or damping of quasi-monochromatic wavepackets propagating in the magnetosphere.

II. TRAJECTORIES OF TEST PARTICLES

Consider a monochromatic whistler wave propagating along a non-uniform external field, $\underset{\sim}{B}_o$, Fig. 1. At any point, z, the wave is described by its vector potential with amplitude A and phase ψ, the latter giving the wave frequency $\omega = \partial\psi/\partial t$ and wavenumber $k = -\partial\psi/\partial z$. If the background plasma is cold, the wave propagates with A = const, ω = const and k given by the cold plasma dispersion relation, $(kc/\omega_p)^2 = (\omega/\omega_p)^2 + \omega/(\Omega - \omega)$. Introducing polar coordinates $(v_\parallel, v_\perp, \varphi)$ for the velocity of the electrons, the equations of motion are[14,15]

$$\frac{dv_\parallel}{dt} = kv_\perp u \sin(\varphi - \psi) - \frac{1}{2} v_\perp^2 \frac{1}{\Omega}\frac{d\Omega}{dz}$$

$$\frac{dv_\perp}{dt} = (\omega - kv_\parallel) u \sin(\varphi - \psi) + \frac{1}{2} v_\parallel v_\perp \frac{1}{\Omega}\frac{d\Omega}{dz} \qquad (2)$$

$$\frac{d\varphi}{dt} = \frac{\omega - kv_\parallel}{v_\perp} u \cos(\varphi - \psi) + \Omega$$

where the external magnetic field is expressed through its gyrofrequency $\Omega(z) = eB_o/mc$ and the wave fields through the reduced vector potential $u = eA/mc$.

The action of the electrons on the wave is expressed by the current, $-e \int d\underset{\sim}{v}\, F v_\perp \exp(i\zeta)$, where $\zeta = \varphi - \psi$ is the phase of the electron velocity relative to the wave vector potential and F is the distribution function of the electrons. This expression for the current, and the pole of the whistler dispersion relation[8] at $v_\parallel = v_r$ indicate that the natural coordinates for resonant interaction are $\theta = k(v_\parallel - v_r)$, $\zeta = \varphi - \psi$ and $v_\perp$. In terms of these coordinates, the equations of motion take the form

$$\frac{d\theta}{dt} = k^2 v_\perp u \sin\zeta - \frac{1}{2}\left[v_\parallel^2\left(\frac{k}{\Omega - \omega} - \kappa\frac{k}{\Omega}\right) - 2v_\parallel + v_\perp^2 \frac{k}{\Omega}\right]\frac{d\Omega}{dz} \quad ,$$

$$\frac{dv_\perp}{dt} = (\Omega - \theta) u \sin\zeta + \frac{1}{2}\left(v_r + \frac{\theta}{k}\right) v_\perp \frac{1}{\Omega}\frac{d\Omega}{dz} \quad , \qquad (3)$$

$$\frac{d\zeta}{dt} = \theta + \frac{(\Omega - \theta)}{v_\perp} u \cos\zeta \quad .$$

Introducing the trapping frequency, $\omega_t = k(v_\perp u)^{1/2}$, the conditions generally satisfied in the magnetosphere,

$$\Omega \sim kv_\perp \sim \omega \sim \Omega - \omega \gg \omega_t \gg ku \quad , \qquad (4)$$

indicate that for resonant interaction, i.e., for $\theta \sim \omega_t$, $\delta t \sim \omega_t^{-1}$, the variations $\delta\theta$ and $\delta(kv_\perp)$ are both of order ω_t, so that $\delta\theta \sim \theta$ while $\delta v_\perp \ll v_\perp$. Therefore one need only be concerned with the equations for ζ and θ, which, in view of the conditions (4), can be approximated by

$$\frac{d}{dt}\zeta = \theta \quad ,$$

$$\frac{d}{dt}\theta = \omega_t^2(R + \sin\zeta) \quad , \qquad (5)$$

where

$$R = -\frac{1}{2}\left[-3v_r + \frac{v_\perp^2 - \kappa v_r^2}{\Omega/k}\right]\frac{d\Omega/dz}{\omega_t^2} \qquad (6)$$

can be called "inhomogeneity ratio", since it gives the magnitude of the external field inhomogeneity in relation to the wave amplitude[11,15]. Both ω_t and R can be treated as constant if the non-uniformity of the external field satisfies

$$\Omega \gg \frac{d\Omega}{dz} v_{\parallel} T \quad , \qquad \frac{d\Omega}{dz} \gg \frac{d^2\Omega}{dz^2} v_{\parallel} T \quad , \tag{7}$$

over the distance, $v_{\parallel}T$, traveled by the electron during the time, T, required to cross the resonance region. It is noted that the last condition requires that the vicinity of the vertex of a parabolic field should be excluded.

It is immediately apparent from Eqs. (5) that, if $|R| < 1$, there exist two equilibrium positions, given by $\theta = 0$ and the two roots of $\sin\zeta + R = 0$. For definiteness we assume from now on that $R > 0$. Then, apart from an additive factor of magnitude 2π, the two equilibrium phase angles, which we denote as ζ_c and ζ_v, are located in the intervals $(-\pi/2, 0)$ and $(\pi, 3\pi/2)$ respectively. It is easy to see that $(\theta = 0, \zeta = \zeta_c)$ corresponds to an unstable equilibrium (saddle point), while $(\theta = 0, \zeta = \zeta_v)$ corresponds to a stable equilibrium (vortex).

The existence of a time-independent vortex suggests the existence, when $|R| < 1$, of a region in the θ-ζ plane in which the trajectories of the particles are represented by closed contours (trapped particles)[12,15]. In order to specify the extent of the trapped region and to further investigate the motion of the particles, the quantity

$$H = 2\omega_t^2 \left[\left(\frac{\theta}{2\omega_t}\right)^2 - \sin^2\frac{\zeta}{2} - R\,\frac{\zeta}{2}\right] \quad , \tag{8}$$

is introduced. It follows from Eqs. (5) that H is an invariant ($dH/dt = 0$), and since $\partial H/\partial\theta = d\zeta/dt$ and $\partial H/\partial\zeta = -d\theta/dt$, H may be considered the Hamiltonian of

the motion. For vanishing external field gradient, $R \to 0$, this invariant reduces to the second invariant[9,16], subject to conditions (4).

From a mathematical point of view, the evaluation of the invariant H reduces the solution of the differential equations, Eqs. (5), to a quadrature: solving Eq. (8) for θ and substituting into the first of Eq. (5) yields the inverse relation $t(\zeta)$,

$$t - t_o = \frac{1}{\omega_t} \int_{\zeta_o/2}^{\zeta/2} \left(\frac{H}{2\omega_t^2} + \sin^2 X + RX\right)^{-1/2} dX \quad , \tag{9}$$

where $t = t_o$ and $\zeta = \zeta_o$ correspond to $\theta = 0$. However, the integral in the right member of Eq. (9) cannot be evaluated in terms of known functions. For $R > 1$, and for $R \leq 1$, in the case of untrapped particles, it can be expressed as an infinite sum involving Bessel functions and Fresnel integrals[12]. For $R \ll 1$, Eq. (9) can be solved and yields $\zeta(t)$ and $\theta(t)$ in terms of elliptic functions, as in the homogeneous case, with an added perturbation due to the weak inhomogeneity represented by R.

In order to use Eq. (8) as an expression, $\theta(\zeta;H)$, for the trajectories of the particles in the ζ,θ plane, it is necessary to remove the periodicity of H with respect to ζ. When $R \leq 1$, this can be done by assigning the value of ζ_o in the interval $\zeta_c \leq \zeta_o < \zeta_c + 2\pi$, where ζ_o is the relative phase angle, ζ, when $\theta = 0$. This choice restricts the Hamiltonian to values satisfying the condition

$$H_v \leq H \leq H_c \quad , \tag{10}$$

where

$$H_v = -2\omega_t^2\left(\sin^2\frac{\zeta_v}{2} + R\,\frac{\zeta_v}{2}\right) \quad ,$$

$$H_c = -2\omega_t^2\left(\sin^2\frac{\zeta_c}{2} + R\,\frac{\zeta_c}{2}\right) \quad .$$

Note that this restriction on permissible values of H is different from that of the homogeneous case: when R = 0 only the trapped particles can reach the value $\theta = 0$, and therefore the corresponding restriction is only $H \geq H_v$.

A set of constant-H curves in the $\theta^2 - \zeta$ plane is shown in Fig. 2a for $R < 1$. The condition (10) imposed on H restricts the acceptable coordinates to a semi-infinite strip, which is bounded by the curves $H = H_c$, $H = H_c'$ and by the ζ-axis (since $\theta^2 \geq 0$), where H_c' is the value of the Hamiltonian at the point $\theta = 0$, $\zeta = \zeta_c + 2\pi$. Since ζ_o is restricted by the inequalities $\zeta_c \leq \zeta_o < \zeta_c + 2\pi$, the curve $H = H_c$ is included in the strip but $H = H_c'$ is excluded; the electrons on $H = H_c'$ being taken into account by $H = H_c$. From the figure it is observed that the condition $\theta^2 \geq 0$ restricts particles located on H_1 or H_2 to oscillate between the $\theta = 0$ points on these curves (trapped particles). This condition does not restrict the particles located on H_3 through H_6. Such particles will eventually advance to $\theta^2 = \infty$ (untrapped particles). The boundary of the two regions, the separatrix, is represented by H_s, which has the same value as H_c' but is within the interval of definition, since it crosses $\theta = 0$ also at $\zeta = \zeta_b$. When the contours of Fig. 2a are represented on the θ-ζ plane, a symmetrical configuration is obtained as shown in Fig. 3a. Thus, when $R < 1$, a trapped-particles region exists extending from $\zeta = \zeta_b$ to $\zeta = \zeta_c + 2\pi$ for $\theta = 0$ and with a maximum width θ_{max} for $\zeta = \zeta_v$. The dependencies of ζ_b, ζ_c and $\theta_{max}/2\omega_t$ on R are plotted in Fig. 4.

When $R > 1$ no real values of ζ_c and ζ_v exist. In order to remove the periodicity of ζ and preserve the continuity near $R = 1$ the limitations on ζ_o must be $-\pi/2 \leq \zeta_o < 3\pi/2$. Correspondingly the permissible values of H are restricted by

$$H_+ \leq H \leq H_- \quad , \tag{11}$$

where

$$H_\pm = -\omega_t^2 \left[\frac{R\pi}{2} + 1 \mp R\pi\right] \quad .$$

In this case, shown in Fig. 2b, the semi-infinite strip in the $\theta^2 - \zeta$ plane is bounded by the curves $H = H_+$, $H = H_-$ and by the ζ-axis. Since no constant-H curve intersects the ζ-axis more than once, all particles are untrapped, eventually advancing to $\theta^2 = \infty$, and no closed trajectories exist in the θ-ζ representation shown in Fig. 3b.

For trapped particles near the vortex, the equations of motion, Eqs. (5), can be linearized and solved to yield the harmonic oscillations[15]

$$\begin{aligned} \zeta(t) &= \zeta_v + (\zeta_o - \zeta_v)\cos\left[(1 - R^2)^{1/4}\,\omega_t t\right] \\ \theta(t) &= -(\zeta_o - \zeta_v)(1 - R^2)^{1/4}\,\omega_t \sin\left[(1 - R^2)^{1/4}\,\omega_t t\right] \end{aligned} \tag{12}$$

where it is assumed that $\theta = 0$ and $\zeta = \zeta_o$ at $t = 0$. The time average of the velocity gives $\langle\theta\rangle = 0$, therefore trapped electrons move with parallel velocities on the average equal to the local wave resonant velocity, $v_r(z)$, while untrapped particles have average parallel velocities, $v_\parallel(z)$, which vary approximately according to cyclotron motion in the non-uniform external field only. Since $v_r(z)$ and $v_\parallel(z)$ vary in opposite direction with respect to z as shown in Fig. 5, the external field gradient causes a separation in velocity space of the trapped and untrapped particles. This behavior of the trapped-electron parallel velocity is accompanied by a deviation of the perpendicular velocity from the values required for conservation of the magnetic moment, $\mu = v_\perp^2/\Omega$. Using the time average $\langle\sin\zeta\rangle = J_o(\zeta_o - \zeta_v)\sin\zeta_v \approx \sin\zeta_v$, where $J_o(x)$ is the Bessel function, the second of Eqs. (3) yields

the rate at which the magnetic moment chages,

$$\frac{d\mu}{dt} = -\frac{1}{2} v_t^2 R \quad , \tag{13}$$

where $v_t = 2\omega_t/k$ is the trapping velocity.

Before concluding this section, it should be pointed out that, ignoring the constant coefficients, Eq. (8) may be interpreted as the conservation of the "energy" H of a particle with "velocity" θ at "position" ζ in a combination of a uniform and a sinusoidal field, with potential $R\zeta/2 + \sin^2\zeta/2$. It follows that a mathematically identical situation would occur in the electrostatic case, with θ and ζ denoting velocity and position and R denoting the amplitude of a uniform external electric field, parallel to the Langmuir wave.

III. PHASE CORRELATION OF A TEST DISTRIBUTION

We consider in this section the evolution of a distribution of test electrons moving in a monochromatic wave, which propagates along a non-uniform external magnetic field.

The propagation of a whistler wave generally does not depend on the detailed dependence of the distribution function on $v_\perp$, but only on the energy moment $\int v_\perp^2 F \, d\underline{v}$. This distribution $F(\underline{v})$ will therefore be chosen initially monoenergetic in the perpendicular direction, with a single value of $v_\perp$ which, however, may depend on $v_\parallel$. In addition, since no preceeding event has modified the distribution, it must be initially uniform with respect to the phase angle φ. Such a distribution can be approximated by

$$F(\underline{v},t) = \sum_{n=-\infty}^{+\infty} F_n(\underline{v},t) \quad , \tag{14}$$

where initially F_n has the shape of a rectangular beam,

$$F_n(\underline{v},t=0) = \frac{q_n}{2\pi v_{\perp n}} \delta(v_\perp - V_{\perp n}) \quad , \quad \text{if} \quad V_{\parallel n} - \frac{1}{2}\Delta v_\parallel < v_\parallel < V_{\parallel n} + \frac{1}{2}\Delta v_\parallel \quad ,$$
$$= 0 \quad , \quad \text{otherwise} \tag{15}$$

where for each beam $q_n \Delta v_\parallel$ is the local density, $V_{\perp n}$ is the perpendicular velocity, $V_{\parallel n}$ is the average parallel velocity and $\Delta v_\parallel$ is the parallel velocity width.

At later times, the effect of the wave fields on the electrons cause the distribution of each beam to acquire a dependence on the phase angle φ, which may be expressed in terms of the amplitude $\bar{C}_n^{(\nu)}$ and phase $\bar{\zeta}_n^{(\nu)}$ of the phase correlation of F_n of order ν, defined by

$$\bar{C}_n^{(\nu)} \exp\left(i\bar{\zeta}_n^{(\nu)}\right) = \langle \exp(i\nu\zeta) \rangle_n \tag{16}$$

where $\zeta = \varphi - \psi(z,t)$, $\psi(z,t)$ is the local phase angle of the wave, defined in Fig. 1a, and the angular bracket denotes an averaging operation over the particles of beam n, $\langle G \rangle_n = \int G(\underline{v}) F_n(\underline{v},t) d\underline{v} / q_n \Delta v_\parallel$. The right member of Eq. (16) is the ν-th order Fourier coefficient of F_n with respect to ζ. The transverse current relative to the wave, which is responsible for wave emissions is given by $j_\perp = \sum_n j_{\perp n}$, where

$$j_{\perp n} = -e q_n \Delta v_\parallel \langle v_\perp \exp(i\zeta) \rangle_n \quad . \tag{17}$$

Writing $v_\perp = \langle v_\perp \rangle_n + \delta v_{\perp n}$, where $\delta v_{\perp n}$ denotes the deviation in an electron perpendicular velocity from the average gives

$$j_{\perp n} = -e q_n \Delta v_\parallel \langle v_\perp \rangle_n C_n^{(1)} \exp\left(i\bar{\zeta}_n^{(1)}\right)$$
$$-e q_n \Delta v_\parallel \langle \delta v_{\perp n} \exp(i\zeta) \rangle_n \quad . \tag{18}$$

From conditions (4) it follows that $|\delta v_{\perp n}| \ll \langle v_\perp \rangle_n$, thus in problems where the distribution functions F_n acquire strong first-order phase correlations, the first term in Eq. (18) is dominant. The computer simulation results of

this section give $\bar{C}_n^{(\nu)}$ and $\bar{\zeta}_n^{(\nu)}$ obtained from Eq. (16), but also include for some cases computations of the magnitude and phase of $j_{\perp n}$ from Eq. (17), therefore allowing an assessment of the significance of $\delta v_{\perp n}$ in Eq. (18). The first-order correlation ($\nu = 1$), which is closely related to the transverse current, is of particular interest in the present study and the simplified notation $\bar{C}_n \equiv \bar{C}_n^{(1)}$, $\bar{\zeta}_n \equiv \bar{\zeta}_n^{(1)}$ will be adopted.

An analytical computation of the transverse current $j_\perp$ would first require an inversion of Eq. (9) to obtain the characteristics of $F_n(v_{\parallel},t)$, followed by a computation of $j_{\perp n}$ from Eq. (17) and finally a summation over n, or the equivalent integration over $v_\parallel$, to obtain $j_\perp$. However, the complexity of Eq. (9) allows this procedure to be followed only in an approximate manner[12]. A numerical approach is used here, with the electrons initialized with a distribution $F_n(v_{\parallel},t=0)$ and the evolution of $F_n(v_{\parallel},t)$ as well as the quantities $\bar{C}_n(t)$ and $\bar{\zeta}_n(t)$ being obtained from the trajectories of individual electrons. The algorithm used to advance the particles is based on the exact set of Eqs. (2) allowing the approximations of Sec. II to be checked. We use the whistler version of the Long-Time-Scale algorithm of Rathmann et al.[13] in which the time step depends on the time scale of the nonlinearities and non-uniformities rather than on the wave or cyclotron frequencies. Since the problem considered here involves weak nonlinearities and non-uniformities, this algorithm is well suited to the solution of this problem.

In the simulations to be presented now, the external magnetic field is given a constant negative gradient $\alpha < 0$, i.e., $\Omega(z) = \Omega_o(1+\alpha z)$, where Ω_o is the gyrofrequency at the center, $z = 0$, of the system of length L, Fig. 5. The wave is chosen with uniform frequency $\omega = \Omega_o/2$, corresponding to a value $k_o c/\omega_p = 1$ at $z = 0$, and with uniform normalized amplitude, $u = 0.25 \times 10^{-6}\ \Omega_o/k_o$.

For this wave, at $z = 0$, $v_{go} = 0.5\ \Omega_o/k_o$ and $v_r = -0.5\ \Omega_o/k_o$. The electrons are initialized within a small distance, Δz, near the boundary at $z = L/2$, with appropriate values of $V_{\parallel n}$ and $V_{\perp n}$ so that, if motion were to occur only under the action of the external field, they would eventually reach the position $z = 0$ with $V_{\parallel no} = v_{ro}$ and with $V_{\perp no} = \Omega_o/k_o$. These values correspond to a trapping frequency $\omega_{to} = 0.5 \times 10^{-3}\ \Omega_o$ and a trapping velocity $v_{to} = 10^{-3}\ \Omega_o/k_o$. A number of computations have been carried out as shown in Tables I and II with different values of the following parameters: α, which governs the value of R; the system length L, so that at the initial position $z = L/2$ the relative velocity $V_{\parallel n} - v_r$ is large enough to suppress any artificial transient correlation; and $\Delta v_\parallel$, in order to obtain information on the mechanism of the superposition of the individual rectangular beams. In all simulations the time step is equal to $\Delta t = 400\ \Omega_o^{-1}$, corresponding to $\omega_{to}\Delta t = 0.2$, and 1333 simulation particles per v_t are used, randomly initialized in $v_\parallel$ and ζ.

(A) Phase correlation when $R < 1$

When $R < 1$, that is, when the non-uniformity of the external field is weak relative to the strength of the wave, the discussion of Sec. II predicts distinct behaviors for trapped and untrapped particles, the extent of the trapping region being given by the quantities ζ_b, ζ_c and θ_{max}, Fig. 4. In particular, if the initial distribution $F_n(v_{\parallel},t=0)$ is taken with $v_r - (V_{\parallel n} + \frac{1}{2}\Delta v_\parallel) > \theta_{max}/k$, no trapped particles exist initially, and therefore no particles are expected to ever become trapped. This should result in the appearance of an empty region inside the separatrix, and, since the electrons cross the resonance line $v_\parallel = v_r$ only within the interval $\zeta_c < \zeta_o < \zeta_b$, a strong correlation is expected when $V_{\parallel n} \approx v_r$, with its phase in the same interval, i.e., $\zeta_c < \bar{\zeta}_n < \zeta_b$.

These expectations are verified by the computer simulations. In Fig. 6 the phase plots are presented in coordinates $\theta/2\omega_t = (v_\parallel - v_r)/v_t$ and $\zeta = \varphi - \psi$, for case 2, corresponding to an initial distribution function F_n with $V_{\parallel n} = v_r - 2v_t$ and $\Delta v_\parallel = 1.5\ v_t$, and an inhomogeneity corresponding to $R = 0.05$. In this case, Fig. 4 gives $\zeta_c = -0.05$, $\zeta_b = 0.76$ and $\theta_{max}/2\omega_t = 0.795$, which are in agreement with the outline of the trapping region in Fig. 6. Furthermore, Fig. 7 shows the build-up of a strong first-order phase correlation, $\bar{C}_n$ associated with a constant phase $\bar{\zeta}_n$. Neglecting a superposed low-amplitude high-frequency oscillation, which is due to the motion of the particles at the $v_\parallel$ - boundaries of the distribution, the amplitude $\bar{C}_n$ reaches a constant value corresponding to $\bar{C}_{max}\Delta v_\parallel/v_t = 0.083$ when most of the particles satisfy the condition $v_\parallel \approx v_r$, while the value $\bar{C}_n = \frac{1}{2}\bar{C}_{max}$ is reached when the leading or the trailing end of the distribution is at $v_\parallel = v_r$, in which case only half of the resonance width is occupied by the electron. Furthermore, when $\bar{C}_n$ is significant (e.g., $\bar{C}_n > 0.25\ \bar{C}_{max}$), the corresponding phase is essentially constant, $\bar{\zeta}_n = 0.2$.

This simulation was repeated, with $\Delta v_\parallel = 3.0\ v_t$ (case 3). Since this time the leading edge of the distribution (at $V_{\parallel n} + \frac{1}{2}\Delta v_\parallel$) is closer to $v_\parallel = v_r$ than the half-width of the separatrix, θ_{max}/k, a small number of electrons are initially trapped and therefore will remain trapped. As is seen in the phase plots of Fig. 8, the distribution function of the untrapped electron evolves generally as in the previous case. Because of the presence of the trapped particles, the separatrix is not delineated when the untrapped particles are near $v_\parallel = v_r$. However, at a later time the untrapped particles move away of the resonance region, while the trapped particles remain inside the separatrix, whose size and shape coincides with that of the previous

case. The amplitude and the phase of the first-order correlations, shown in Fig. 9, have essentially the same features as in Fig. 7: the amplitude reaches in effect the same maximum value, $\bar{C}_{max}\Delta v_\parallel/v_t = 0.081$, the value $\bar{C}_n = 1/2\ \bar{C}_{max}$ appears when $v_\parallel = v_r$ for the leading or trailing ends of the distribution, and the larger values of $\bar{C}_n$ are accompanied by a constant phase $\bar{\zeta}_n = 0.2$, showing that the observed phase correlation is independent of the beam width. The correlation in this case lasts for a longer time, corresponding to the longer time required for the beam to cross the trapping region.

In order to verify that the correlation observed so far is primarily due to the absence of trapped particles, the simulation with $R = 0.05$ is repeated, this time with $V_{\parallel n} = v_r$ and $\Delta v_\parallel = 3\ v_t$ (case 4). This choice guarantees that the trapped-particle region is initially filled with particles, which remain trapped and move with average velocity v_r. It is indeed observed in Fig. 10 that the initially untrapped particles gradually move away from the resonance region and eventually form a beam at $v_\parallel - v_r \gg v_t$, covering all values of ζ, while the initially trapped particles remain to form an island inside the separatrix. The amplitude of the first-order correlation, Fig. 11a, initially has some transient oscillations, which are related to the wavy motion of the velocity boundaries of the distribution. Later, when the untrapped particles move away from the resonance region and become approximately uniformly distributed in phase, the correlation of the trapped particles produces a constant $\bar{C}_n$, corresponding to a value $\bar{C}_n\Delta v_\parallel/v_t = 0.123$, of the same order as in the previous cases. At the same time, the phase of the correlation, given in Fig. 11b, remains approximately constant at the value $\bar{\zeta}_n = -3.0$. This value differs by half a revolution from the corresponding value of the previous

simulations, as expected, since the correlation in that case was due to a hole rather than an island in the trapped-particle region.

Further simulations have been performed with a variety of values for $R < 1$ and $\Delta v_\parallel / v_t$, as shown in Table I. The results indicate that if $\Delta v_\parallel / v_T \geq 1.5$, the correlation reaches a maximum value corresponding to $\bar{C}_n \Delta v_\parallel / v_t \sim 0.1$, essentially independent of $\Delta v_\parallel / v_t$ and with a weak dependence on R. These values are shown in Fig. 12 by the circles and dots, depending on whether the correlation is produced by a hole or an island. For smaller ratios $\Delta v_\parallel / v_t$, especially when $\Delta v_\parallel / v_t < 0.5$, the correlation amplitude per velocity width decreases sharply. This indicates that a distribution with width $\Delta v_\parallel \sim 1.5\, v_t$ eventually uses all the available resonance width. The simulations also indicate that for $R < 1$, as long as $\bar{C}_n$ is large, the phase of the correlation with respect to the wave remains constant but with a value depending on the value of R. The values $\bar{\zeta}_n(R)$ observed in the simulations are shown in Fig. 4 by the circles or dots for the cases of a hole or an island, respectively. In all simulations, no significant correlation of order higher than the first has been observed, except for narrow distributions with widths $\Delta v_\parallel / v_t \leq 0.5$. Finally, computations of the transverse current $j_{\perp n}$ show that the correction due to $\delta v_{\perp n}$ in Eq. (18) is insignificant for the wave amplitude and perpendicular velocity considered here which gives $v_t / v_\perp = 10^{-3}$.

The phase correlation may be estimated analytically for cases, such as case 4, in which the trapping region is initially occupied. After sufficiently long times, the untrapped electrons move to velocities $v_\parallel - v_r \gg v_t$ and become uniformly distributed in the interval $0 < \zeta < 2\pi$, as shown in Fig. 9, while the trapped electrons remain within the separatrix and may be assumed to be uniformly distributed within this region. Assuming that the expression

$$\frac{v_\parallel - v_r}{v_t} = \frac{\theta_{max}}{2\omega_t} \cos[\pi(\zeta - \zeta_{av})/2\Delta\zeta] \quad , \tag{19}$$

defined in $|\zeta - \zeta_{av}| \leq \Delta\zeta$, where $\zeta_{av} = (\zeta_c + 2\pi + \zeta_b)/2$, and $\Delta\zeta = (\zeta_c + 2\pi - \zeta_b)/2$, is a reasonable approximation for the separatrix, Eq. (14) yields

$$\bar{C}_n = \frac{v_t}{\Delta v_\parallel} \frac{\theta_{max}}{2\pi\omega_t} \frac{\Delta\zeta \cos \Delta\zeta}{(\pi/2)^2 - (\Delta\zeta)^2} \tag{20}$$

and $\bar{\zeta}_n = \zeta_{av}$. Using the values of $\theta_{max}/2\omega t$, ζ_b and ζ_c as functions of R given in Fig. 5 yields the asymptotic values of $\bar{C}_n$ plotted in Fig. 12. This estimate may also be applied to the case of a hole (e.g. case 2) if a uniform distribution of untrapped particles is assumed in the θ-ζ plane. In this case Eq. (20) remains valid and $\bar{\zeta}_n = \zeta_{av} - \pi$. The data points for $\bar{C}_n$ in Fig. 12 and for $\bar{\zeta}_n$ in Fig. 5 match satisfactorily the above analytical estimates, both in order of magnitude and in trend.

(B) Phase correlation when $R > 1$

For sufficiently strong non-uniformity of the external field, corresponding to $R > 1$, the analysis of Sec. II shows that particle trapping is not possible. However, the trajectories of individual particles do not give for this case any direct information about their collective behavior, e.g., the generation of a phase correlation or coherent transverse current.

A situation of this type is provided by case 18, where $R = 2.5$, and initial values $V_{\parallel n} = v_r - 7v_t$ and $\Delta v_\parallel = 6v_t$. The phase plots of Fig. 13 indicate the generation of a fine structure, produced by the ζ-dependence of the acceleration $d\theta/dt$. The presence of any phase correlation is not apparent in the phase plots, but the Fourier analysis of the distribution reveals a first-order correlation with a magnitude $\bar{C}_n(t)$, having two maxima

centered at $t_1 \simeq 8 \times 10^3\ \Omega_o^{-1}$ and $t_2 \simeq 1.7 \times 10^4\ \Omega_o^{-1}$ separated by smaller values, see Fig. 14a. Comparison with the phase plots of Fig. 13 shows that these maxima correspond to the passage of the two boundaries of the distribution function at $v_\parallel = v_r$. The maxima of $\bar{C}_n$ are also accompanied by rapid variations in the phase $\bar{\zeta}_n$ shown in Fig. 14b. This variation of the phase is essentially linear, at a rate $\omega_t^{-1} d\bar{\zeta}_n/dt = 1.9$, and coincides with the average phase angle of the fine structure of the phase plots near $v_\parallel = v_r$. Since this fine structure is associated with the abrupt boundaries of the initial distribution $F_{n\infty}(v)$ at $v_\parallel = V_{\parallel n} \pm 0.5\ \Delta v_\parallel$, phase correlation in the present case would be expected only from distribution functions having steep gradients with respect to $v_\parallel$.

Repeating this simulation with different values of the ratio $\Delta v_\parallel / v_t$ confirms that the phase correlation in the present case, $R = 2.5$, is indeed associated with boundary effects. For a narrower beam with $\Delta v_\parallel \simeq 3\ v_t$ (case 17) the fine structure extends across the width of the beam and the two maxima of $\bar{C}_n$ merge into a single broader maximum as shown in Fig. 15a, while the phase of the correlation, $\bar{\zeta}_n$ increases linearly with time (Fig. 15b), at a rate $\omega_T^{-1} d\bar{\zeta}_n/dt = 1.4$, without interruption. For a wider beam with $\Delta v_\parallel = 12\ v_t$ (case 19), the maxima of $\bar{C}_n$ are further apart, corresponding to the longer time between passage of the boundary fine structures across $v_\parallel = v_r$. Other simulations with $R = 1.25$ show qualitatively similar results.

In all simulations with $R > 1$, the correlation associated with the abrupt $v_\parallel$-boundaries is accompanied by a linear variation of the phase, at a rate

$$\frac{d\bar{\zeta}_n}{dt} \sim R\omega_t \quad . \tag{21}$$

It can be seen that this correlation is coherent to a satellite wave with frequency $\omega + \delta\omega$ where

$$\delta\omega \sim \frac{R\omega_t}{1 + \frac{\Omega}{2\omega}} \quad . \tag{22}$$

Thus, a whistler wave acting on a distribution with steep gradients in the parallel velocity is expected to give rise to direct growth of sidebands.

IV. *DISCUSSION*

The numerical results of the preceeding section show that for $R \leq 0.8$, a set of electrons initially located at A in the $z - v_\parallel$ plane, as shown in Fig. 5, under the action of a monochromatic whistler wave propagating in a non-uniform magnetic field, becomes correlated in phase as it crosses the resonant velocity v_r at A', then loses its correlation as it moves on to A".

The phase correlation at A' results from a hole in the $\zeta - v_\parallel$ plane corresponding to the trapping region which moves at the velocity v_r, while the surrounding untrapped electrons follow approximately a cyclotron motion in the non-uniform external field only. The phase correlation was shown to be independent of the width $v_\parallel$, provided that $\Delta v_\parallel \geq 1.5\ v_t$.

Consider now a beam of electrons with parallel velocities between $V_\parallel$ and $V_\parallel + \Delta v_\parallel$, extending over the entire length L of the system, and which is in equilibrium under the action of the external magnetic field only. Such a beam may be considered as a series of sets of electrons $A_1, A_2, \ldots$ as shown in Fig. 16. These sets move (to the left in Fig. 16) according to pure cyclotron motion and become correlated in phase only during their passage through the interval $(z, z + \Delta z)$. If we assume that the trapping region in the interval $(z, z + \Delta z)$ is not initially occupied by electrons, this trapping region remains empty and a constant phase correlation is maintained in the interval $(z, z + \Delta z)$. By superposition of a set of such beams, it follows that

a distribution of electrons covering the entire $z - v_\parallel$ plane, but excluding the trapping region located along the line $v_\parallel = v_r$, must give a phase correlation uniform with respect to z and constant in time.

In an actual situation involving magnetospheric whistlers, one deals with a wavepacket whose leading front is expected to trap electrons as it advances into the unperturbed plasma, and the trapping region behind the front is not empty. However, it can be shown that the trapped electrons generally have a different density than the surrounding untrapped electrons. Consider a semi-infinite wave with an abrupt leading front, which at time t is located at position z_f and moves to the right (Fig. 17). At position z and time t (Point A), the correlated untrapped electrons are those originating at z_o, $v_\parallel = V_\parallel(z_o)$ (Point A'), where z_o is an arbitrary reference position. At the same time, trapped electrons at z are those which have been captured at an earlier time t' by the wave front located at z_f' (Point B) and have moved from B to A along the trajectory $v_\parallel = v_r$. Prior to being trapped these electrons have moved according to pure cyclotron motion and therefore they originate at z_o, $v_\parallel = V_\parallel(z_o) + \delta V_\parallel$ (Point B'). The velocity interval $\delta V_\parallel$ is evaluated by noting that during the time interval t - t', trapped electrons move a distance $z - z_f' \approx (t - t')v_r$, while the wave front moves a distance $z_f - z_f' \approx (t - t')v_g$, from which, using also the second of Eqs. (5),

$$\delta V_\parallel \approx \frac{1}{2} R\omega_t \frac{v_t}{v_g - v_r} (z_f - z) \quad . \tag{23}$$

Because of the velocity interval $\delta V_\parallel$, the local density of the trapped electrons is generally different from q, the density of the untrapped electrons, by the amount

$$\delta q \approx q \frac{1}{F} \frac{\partial F}{\partial v_\parallel}\bigg|_{v_\parallel = V_\parallel} \delta V_\parallel \quad . \tag{24}$$

In addition, at position z, the perpendicular velocity of the untrapped electrons, $V_\perp$, is different from that of the trapped electrons, $V_\perp + \delta V_\perp$. This difference is given by

$$\delta V_\perp \approx \frac{\partial V_\perp}{\partial v_\parallel}\bigg|_{v_\parallel = V_\parallel} \delta V_\parallel + \frac{1}{2} V_\perp \frac{\delta \mu}{\mu} \quad , \tag{25}$$

where the first term represents the dependence of the r.m.s. perpendicular velocity on the parallel velocity, e.g., in the case of a loss-cone distribution, while the second term accounts for the variation of magnetic moment of the trapped particles, given by Eq. (13).

Using the equation[13]

$$\frac{d\mathcal{U}}{dt} \equiv \frac{\partial \mathcal{U}}{\partial t} + v_g = -\epsilon \frac{(\Omega - \omega)^2}{\Omega} \langle v_\perp \sin \zeta \rangle$$

where ϵ gives the ratio of the number of particles, over which the average is taken (i.e., the resonant particles), to the total number of particles, the nonlinear growth rate, $\gamma_{NL} = (d\mathcal{U}/dt)/\mathcal{U}$, can be expressed by

$$\gamma_{NL} = q\Delta v_\parallel V_\perp \bar{C} \sin \bar{\zeta} \left(\frac{\delta q}{q} + \frac{\delta V_\perp}{V_\perp}\right) \frac{(\Omega - \omega)^2}{\Omega \mathcal{U} N} \tag{26}$$

where $\bar{\zeta}$ is the average phase of the untrapped resonant electrons and N is the electron density. From Eqs. (13) and (23) to (25) one can obtain

$$\frac{\delta q}{q} + \frac{\delta V_\perp}{V_\perp} = -\frac{R\Omega\omega_t^2 (z_f' - z)}{kV_\perp^2 (\Omega - \omega)} \left[1 - \frac{1}{2} \frac{k}{\Omega q} \frac{\partial}{\partial v_\parallel} (V_\perp^2 q)\right]_{v_\parallel = v_R} .$$

Then, using the expression for the linear growth rate, which in this case is

$$\gamma_L = -\pi \frac{(\Omega - \omega)^2}{k} \frac{q}{N} \left[1 - \frac{1}{2} \frac{k}{\Omega q} \frac{\partial}{\partial v_\parallel} (V_\perp^2 q)\right]_{v_\parallel = v_R} ,$$

and using the estimates $\bar{C} = 0.1\, v_t/\Delta v_{\parallel}$ and $\sin \bar{C} = R$, supported by the computations of Sec. III when $R \leq 0.6$, gives

$$\frac{\gamma_{NL}}{\gamma_L} = \frac{1}{5\pi} R^2 \frac{\omega_t (z_f - z)}{v_g - v_r} \quad . \tag{27}$$

Except for the leading numerical coefficient, this result agrees with the analysis of Karpman et al. (see Eq. 4.30 or 5.8 of Ref. 17), under the assumption of essentially constant amplitude, inherent in the present discussion.

In order to give a concrete assessment of the significance of Eq. (26), we conclude with a simple numerical calculation of the growth rate at a position corresponding to 150 msec inside a key-down 40 mγ and 5.6 kHz pulse. The inhomogeneity of the external field is taken to correspond to the geomagnetic lines with $L \approx 4$ to 4.5 at positions 1 to 2 Earth radii away from the equatorial plane, where $\Omega \approx 9 \times 10^4$ sec^{-1} and $d\Omega/dz \approx 8 \times 10^{-5}$ (cm sec)$^{-1}$. The cold electrons are assumed with a density $N \sim 400$ cm^{-3} and the distribution of the energetic electrons is assumed to be bi-Maxwellian, with density 4×10^{-2} cm^{-3}, with perpendicular and parallel thermal velocities $v_{\perp th}$ and $v_{\parallel th}$ respectively. For $v_{\perp th}/c \approx 0.1$, the r.m.s. perpendicular velocity $V_{\perp} = \sqrt{2}\, v_{\perp th} \approx 1.5\, \Omega/k$ gives $\omega_t \approx 10^3$ sec^{-1} and $R \approx 0.5$. Assuming $v_{\perp th}/v_{\parallel th} \approx 2$, the linear growth rate is $\gamma_L \approx 6$ sec^{-1} and Eq. (27) gives $\gamma_{NL} \approx \gamma_L$. Applying this growth rate for a time of 0.5 sec during which the wave travels a distance of 1.1 Earth radius gives a magnification by a factor of $e^3 = 20$.

Although the nonlinear and linear growth rates are approximately equal in the preceding example, it should be noted that γ_{NL}, which is associated with the non-uniformity of the external field corresponds to a different instability mechanism than the linear growth rate γ_L. In a uniform magnetic field, the large-amplitude conditions $\omega_t \gg \gamma_L$, satisfied in the example, would imply

that no growth could occur, since the ergodic state is approached within a time ω_t^{-1}, shorter than the growth time γ_L^{-1}. However, in a non-uniform magnetic field, the continuous influx of fresh untrapped particles prevents the ergodization, and the wave is expected to grow even for large amplitudes satisfying the condition $\omega_t \gg \gamma_{NL}$.

The self-consistent problem, in which the amplitude and frequency of the wavepacket are allowed to vary under the action of the correlated electrons, is beyond the scope of this paper. Computer simulations of this problem, currently being studied, will be the subject of a future paper.

ACKNOWLEDGEMENTS

This work is supported by the Office of Naval Research under contract N00014-75-C-0473. Acknowledgement is made to the National Center for Atmospheric Research, which is sponsored by the National Science Foundation, for computer time used in this research. This research was conducted in cooperation with R. N. Sudan, whose work is supported by the Atmospheric Sciences Division of the National Science Foundation under grant ATM75-02797A01.

REFERENCES

1. J. Denavit and R. N. Sudan, Phys. Rev. Lett. 28, 404 (1972).
2. J. Denavit and R. N. Sudan, Phys. Fluids 18, 1533 (1975).
3. N. Sato, K. Saeki and R. Hatakeyama, Phys. Rev. Lett. 38, 1480 (1977).
4. R. A. Helliwell, J. Katsufrakis, M. Trimpi and N. Brice, J. Geophys. Res. 69, 2391 (1964).
5. I. Kimura, J. Geophys. Res. 73, 445 (1968).
6. R. N. Sudan and J. Denavit, Phys. Today 26, No. 12, 32 (1973).
7. U. S. Inan, T. F. Bell, D. L. Carpenter and R. R. Anderson, J. Geophys. Res. 82, 1177 (1977).
8. R. N. Sudan, Phys. Fluids 6, 57 (1963); T. F. Bell and O. Buneman, Phys. Rev. 133, A1300 (1964).
9. P. Palmadesso and G. Schmidt, Phys. Fluids 14, 1411 (1971).
10. S. L. Ossakow, E. Ott and I. Haber, Phys. Fluids 15, 2314 (1972).
11. K. B. Dysthe, J. Geophys. Res. 76, 6915 (1971).
12. V. I. Karpman, J. N. Istomin and D. R. Shklyar, Phys. Scr. 11, 278 (1975).
13. C. E. Rathmann, J. L. Vomvoridis and J. Denavit, J. Comput. Phys. 26, 408 (1978).
14. R. N. Sudan and E. Ott, J. Geophys. Res. 76, 4463 (1971).
15. D. Nunn, Planet. Space Sci. 22, 349 (1974).
16. R. F. Lutomirski and R. N. Sudan, Phys. Rev. 147, 156 (1966).
17. V. I. Karpman, Ja. N. Istomin and D. R. Shklyar, Plasma Phys. 16, 685 (1974).

Case	R	$\frac{V_{\parallel n} - v_r}{v_t}$	$\frac{\Delta v_\parallel}{v_t}$	$\bar{C}_n \frac{\Delta v_\parallel}{v_t}$	$\bar{\zeta}_n$
1	0.05	-1.5	1.5	0.078	0.2
2		-2	1.5	0.083	0.2
3		-2	3.0	0.081	0.2
4		0	3.0	0.123	-3.0
5	0.25	-3	1.5	0.072	0.8
6		-3	3.0	0.105	0.7
7		0	3.0	0.125	-2.6
8	0.6	-4	3.0	0.057	1.8
9		-4	6.0	0.075	1.3
10		0	6.0	0.084	-1.7
11	0.8	-4	3.0	0.072	2.1
12		-4	6.0	0.048	2.2
13		0	6.0	0.060	-1.5
14	0.95	-4	3.0	0.072	2.7
15		-4	6.0	0.039	2.8
16		0	6.0	0.054	-1.0

Table I. Computer simulations for R < 1.

Case	R	$\frac{V_{\parallel n} - v_r}{v_t}$	$\frac{\Delta v_\parallel}{v_t}$	$\bar{C}_n \frac{\Delta v_\parallel}{v_t}$	$\frac{1}{\omega_T} \frac{d\bar{\zeta}_n}{dt}$
17	1.25	- 5	1.5	0.102	1.12
18		- 5	3.0	0.099	0.68
19	2.5	- 7	1.5	0.088	1.84
20		- 7	3.0	0.084	1.40
21		- 7	6.0	0.072	1.94
22		-13	12.0	0.072	1.35

Table II. Computer simulations for R > 1.

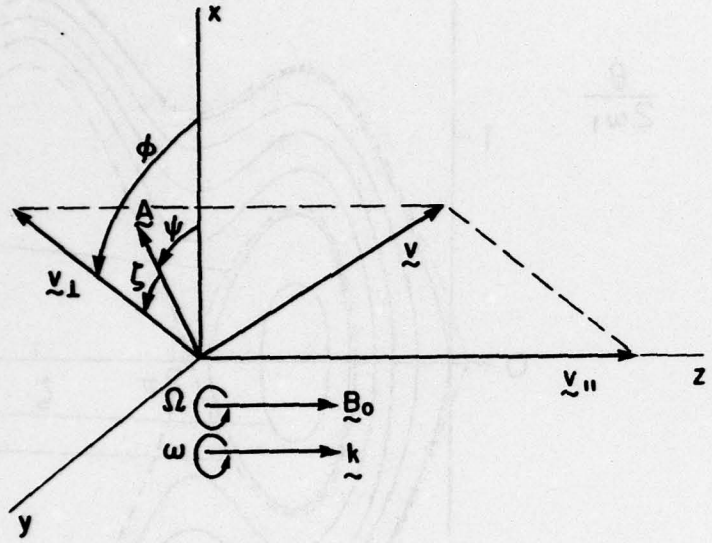

Figure 1. Geometry of the whistler wave and the electron velocity.

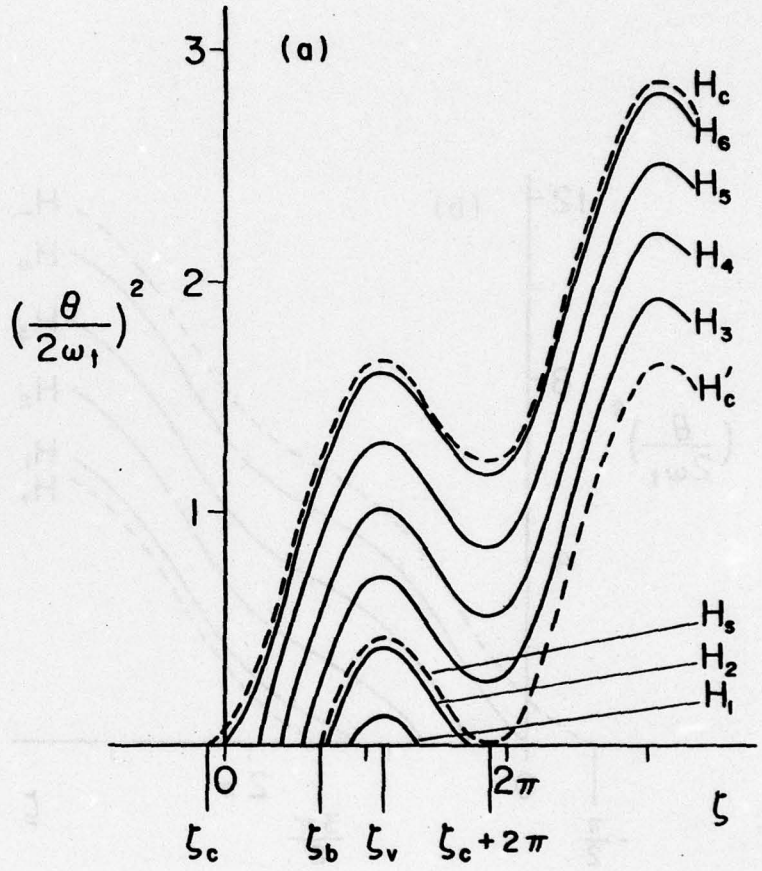

Figure 2a. Curves of constant H for $|R| < 1$. The curves are scaled to correspond to R = 0.382.

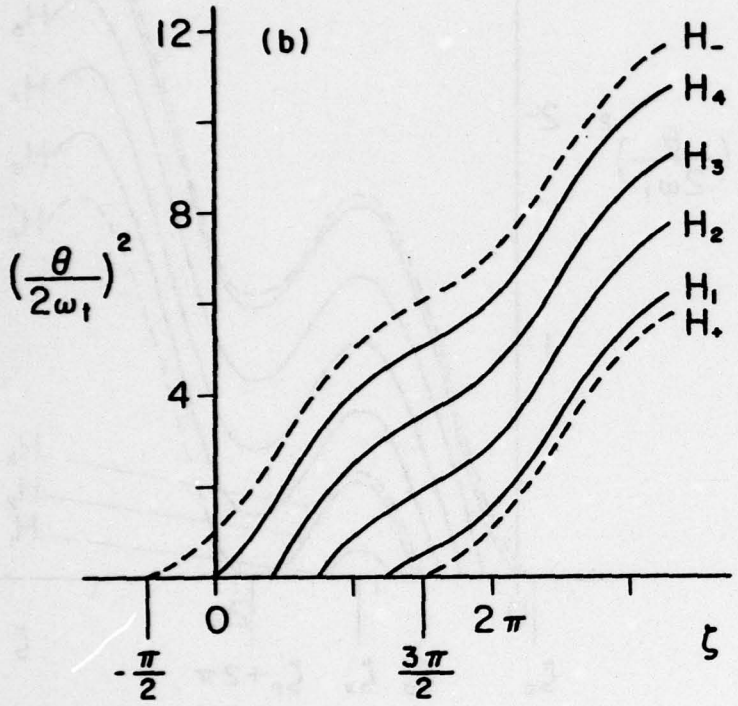

Figure 2b. Curves of constant H for $|R| > 1$. The curves are scaled to correspond to $R \approx 1.91$.

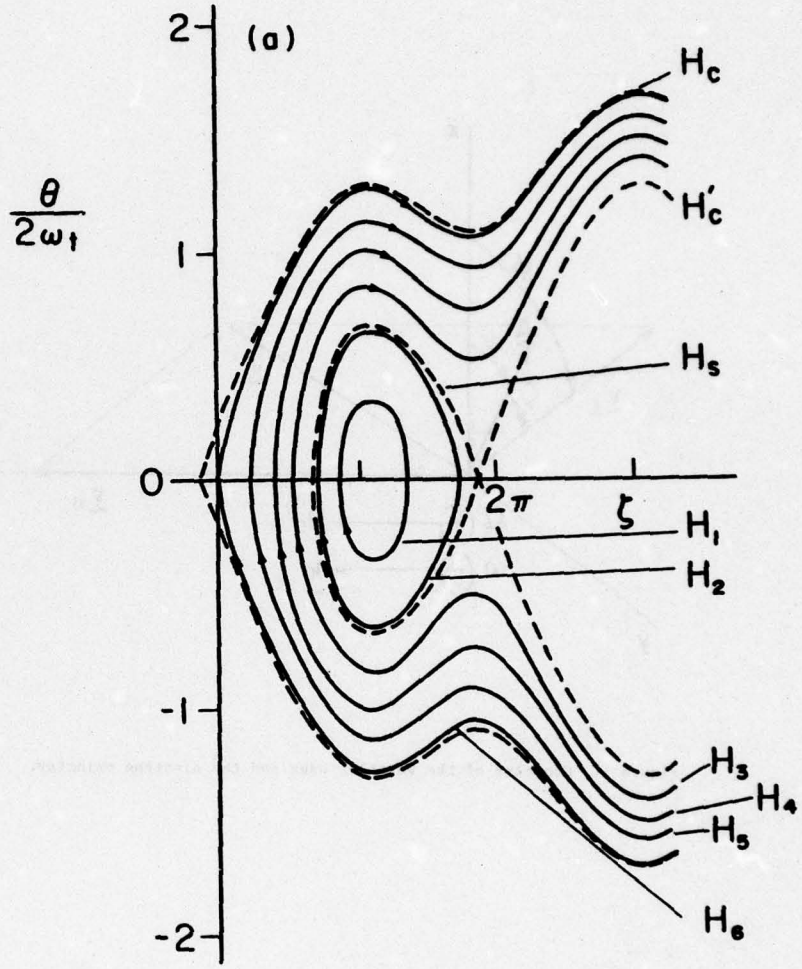

Figure 3a. Trajectories in a whistler wave and a non-uniform field for the case of Fig. 2a for $|R| < 1$.

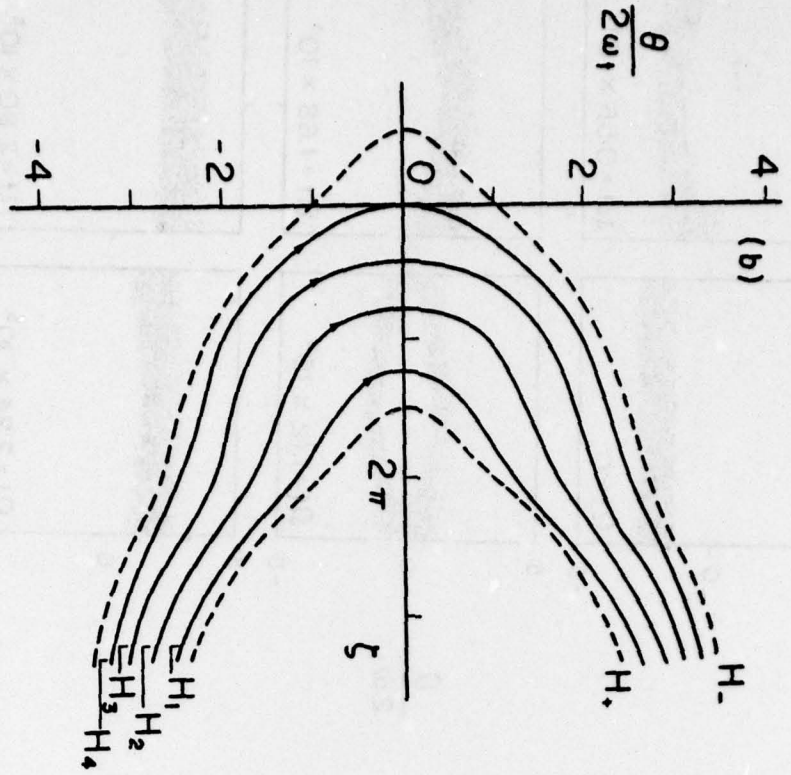

Figure 3b. Trajectories in a whistler wave and a non-uniform field for the case of Fig. 2b for $|R| > 1$.

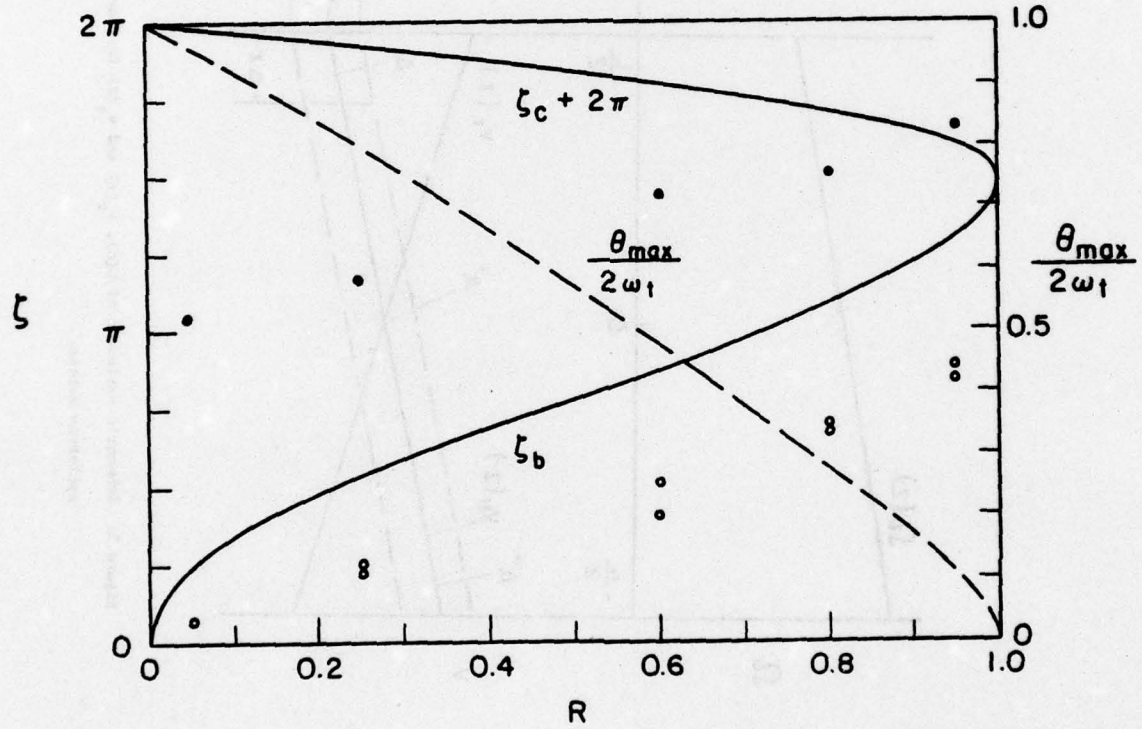

Figure 4. Dependence on R of ζ_b, ζ_c and $\theta_{max}/2\omega_t$. Phase angle of the correlation (Sec. III) in the cases of a hole (circles) and of an island (dots).

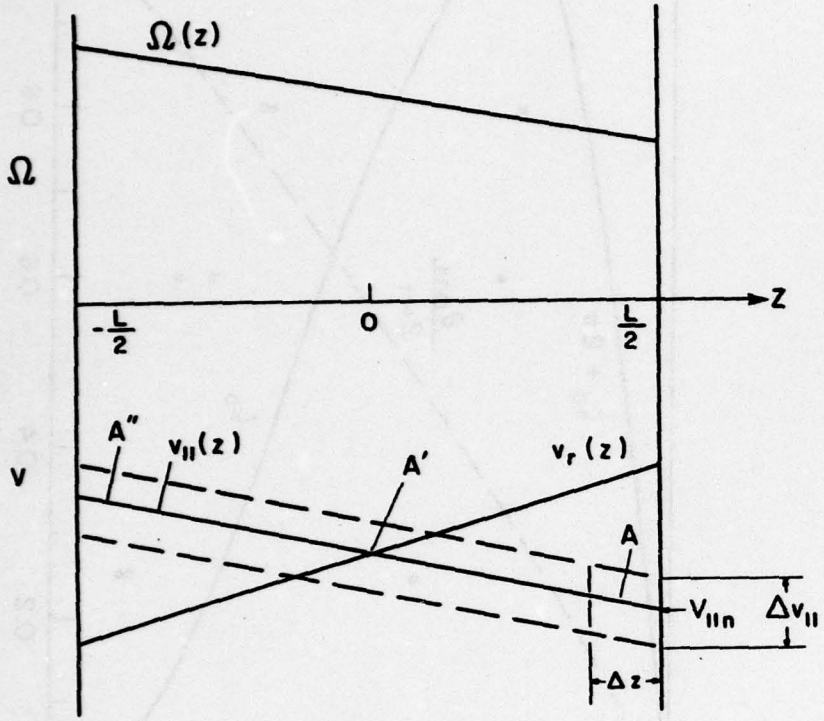

Figure 5. Schematic variation of $\Omega(z)$, $v_r(z)$ and $v_\parallel(z)$ for pure cyclotron motion.

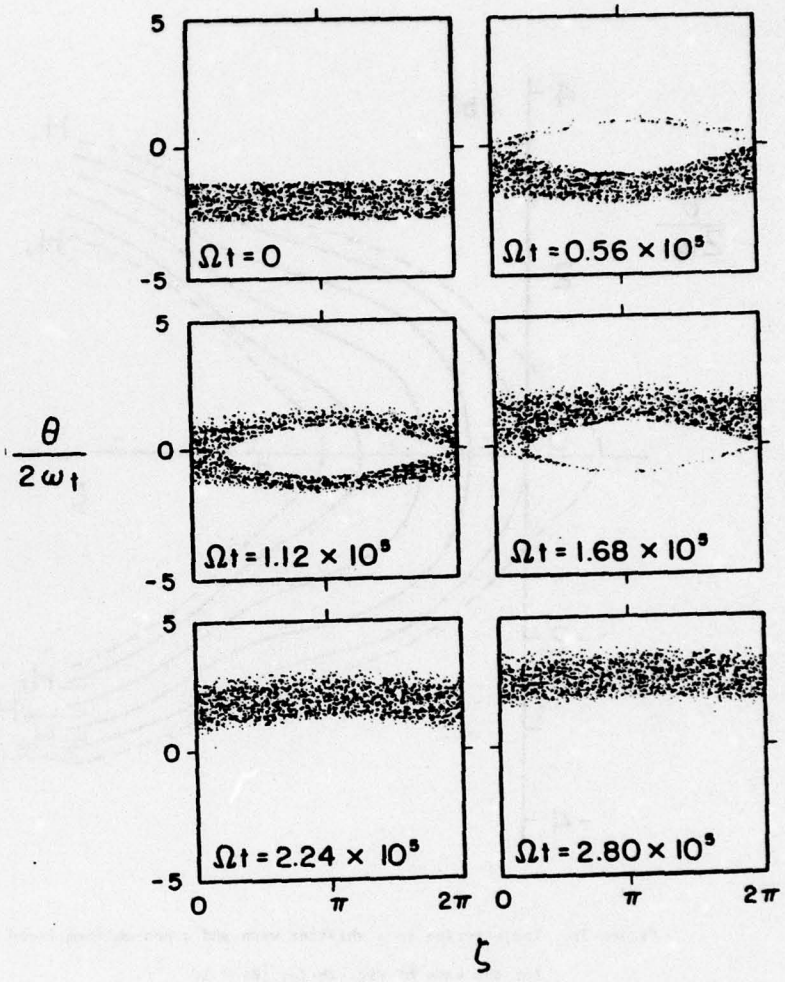

Figure 6. Phase plots for the case $R = 0.05$, $\Delta v_\parallel = 1.5\, v_t$ and $v_{\parallel n} = v_r - 2\, v_t$ initially.

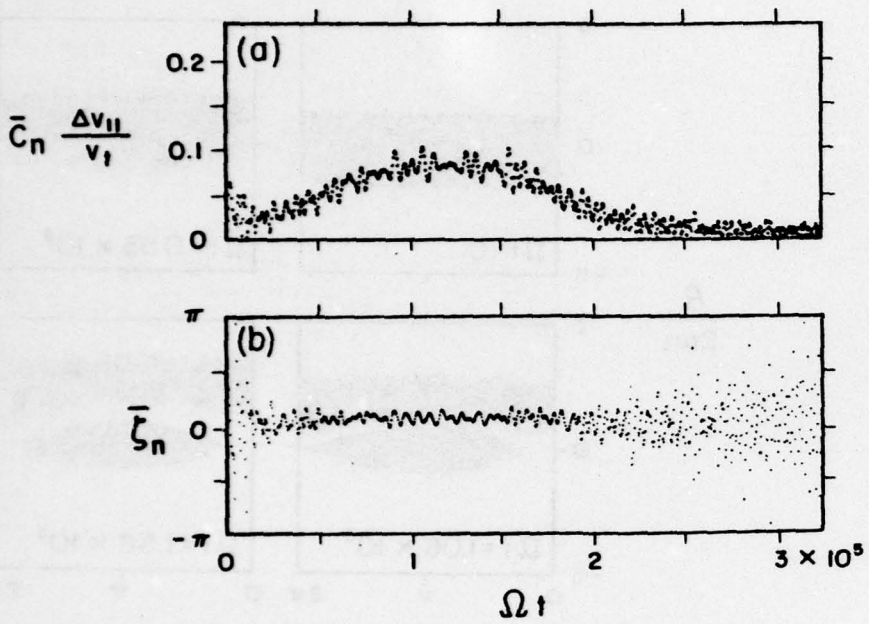

Figure 7. Amplitude, $\bar{C}_n$, and phase, $\bar{\zeta}_n$, of the correlation for the simulation of Fig. 6.

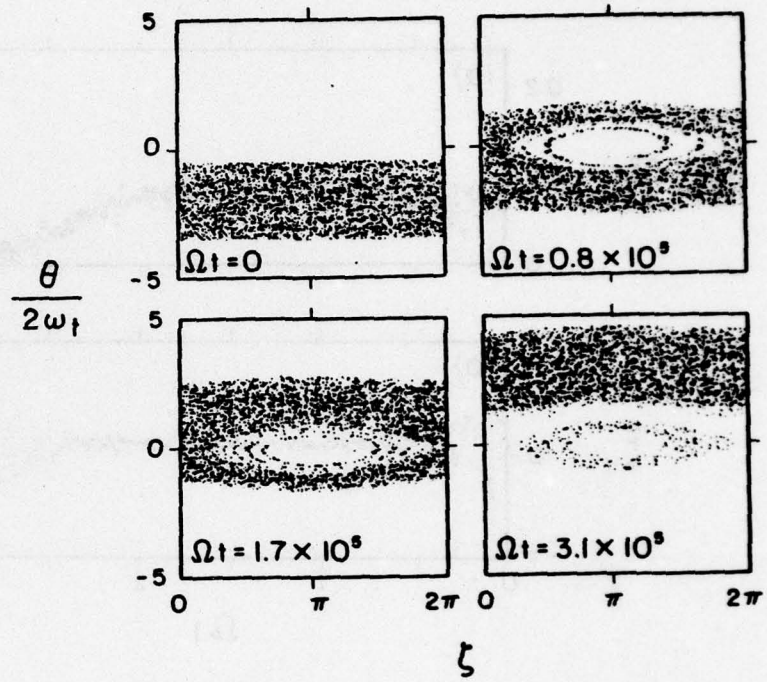

Figure 8. Phase plots for the case R = 0.05, $\Delta v_{||} = 3.0\ v_t$ and $v_{||n} = v_r - 2\ v_t$.

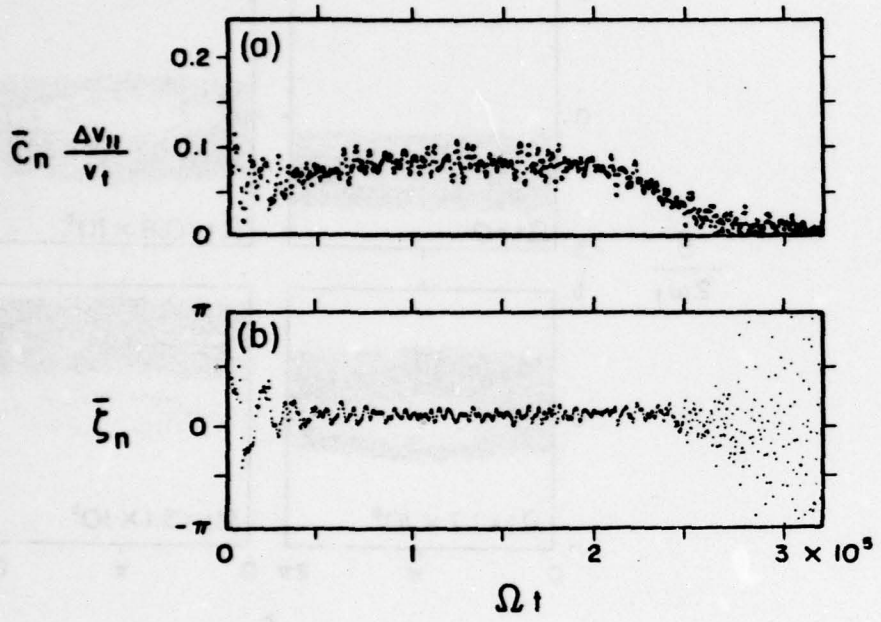

Figure 9. Amplitude, $\bar{C}_n$, and phase, $\bar{\zeta}_n$, of the correlation for the simulation of Fig. 8.

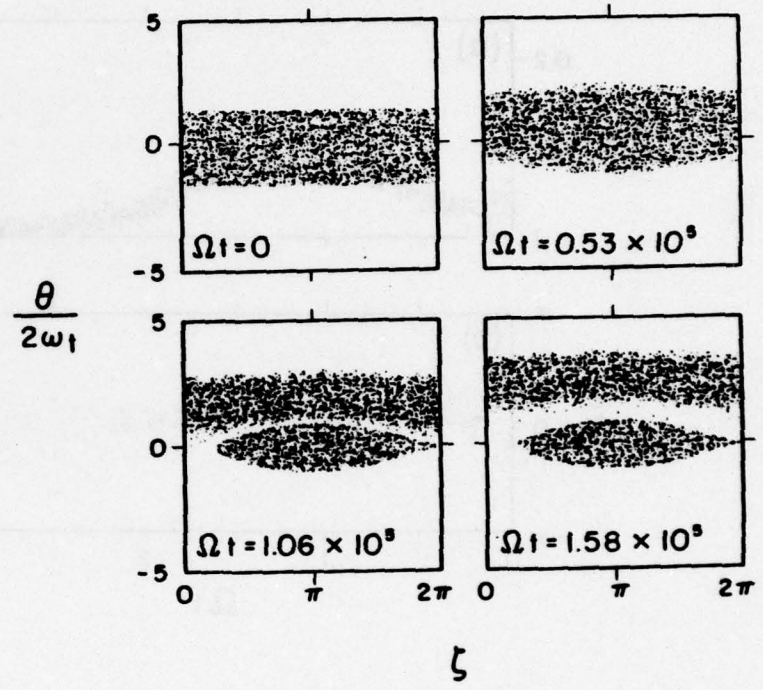

Figure 10. Phase plots for the case R = 0.05, $\Delta v_{\parallel} = 3\, v_t$ and $V_{\parallel n} = v_r$ initially.

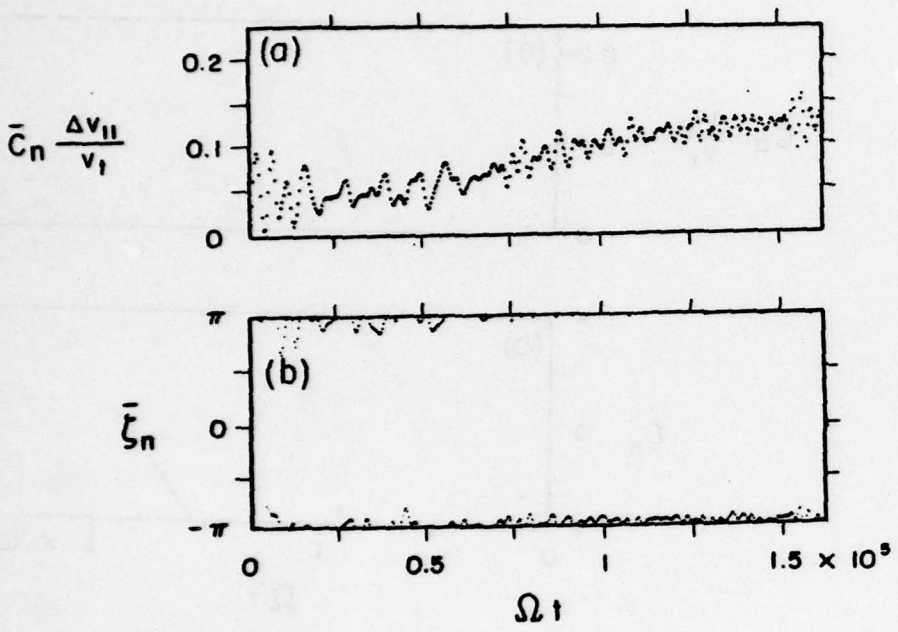

Figure 11. Amplitude, $\bar{C}_n$, and phase, $\bar{\zeta}_n$, of the correlation for the simulation of Fig. 10.

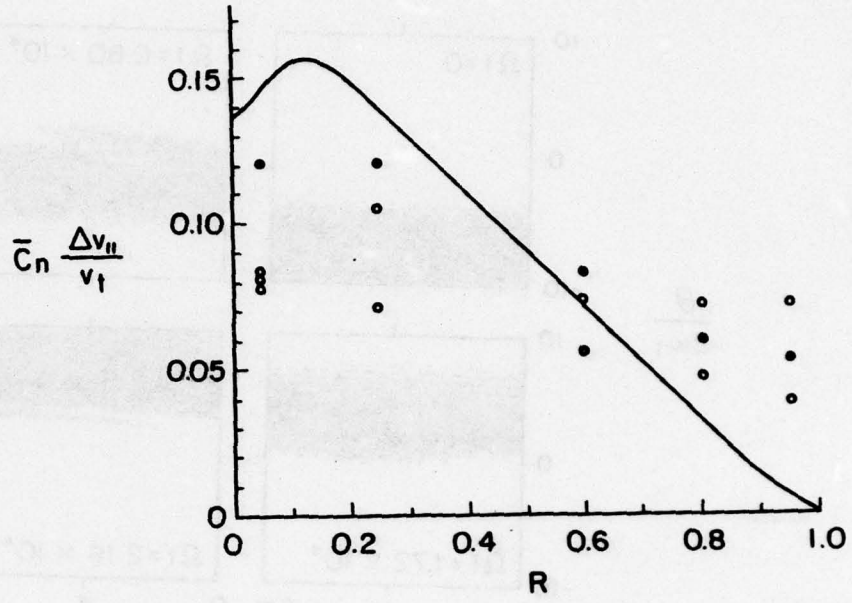

Figure 12. Amplitude of the correlation when $R < 1$ in the cases of a hole (circle) and of an island (dots). The solid line gives the analytic estimate of $\bar{C}_n$, given in Eq. (20).

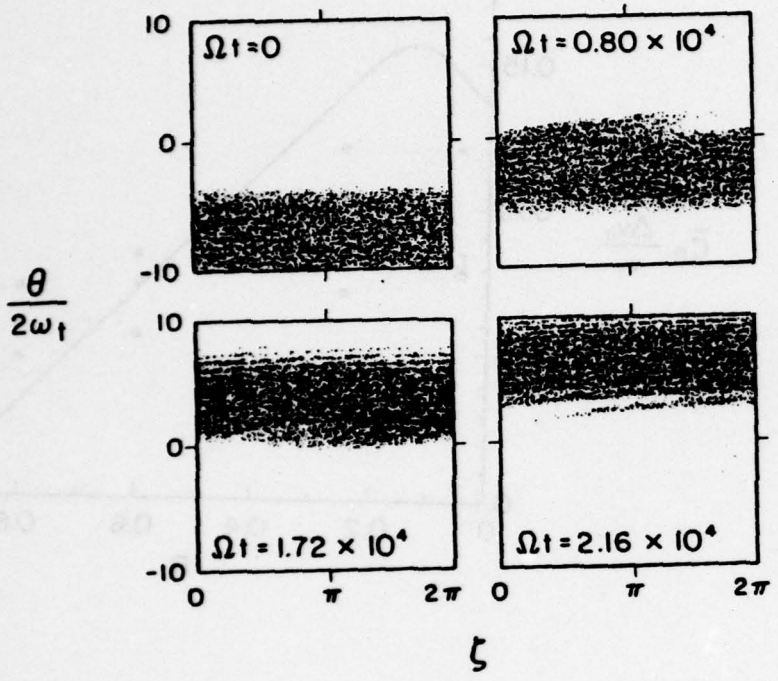

Figure 13. Phase plots for the case R = 2.5, $\Delta v_{\parallel} = 6\ v_t$ and $V_{\parallel n} = v_r - 7\ v_t$ initially.

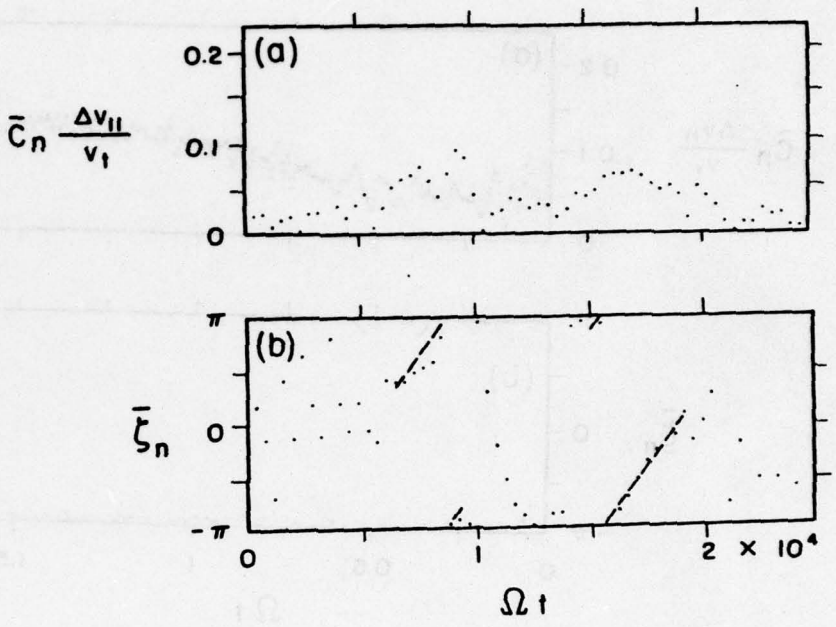

Figure 14. Amplitude, $\bar{C}_n$, and phase, $\bar{\zeta}_n$, of the correlation for the simulation of Fig. 13.

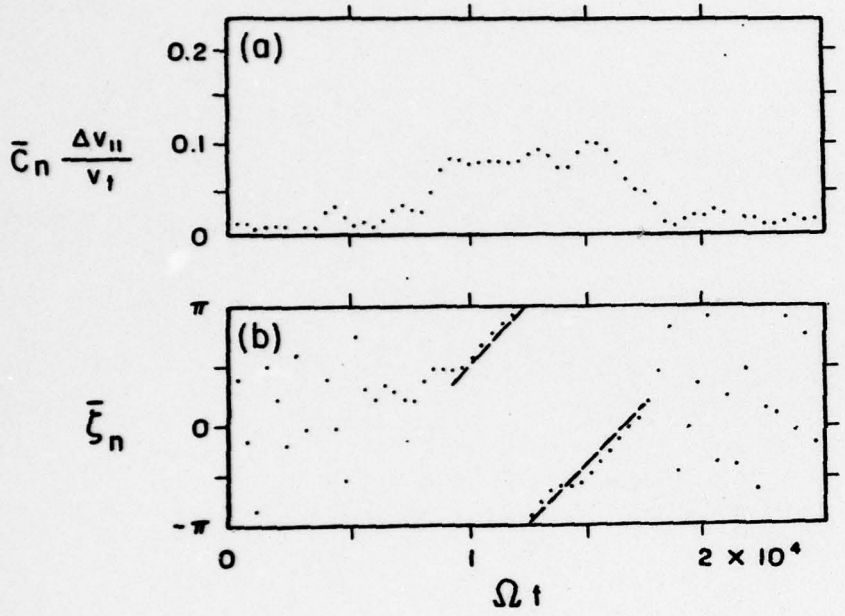

Figure 15. Amplitude, $\bar{C}_n$, and phase, $\bar{\zeta}_n$, of the correlation for the case R = 2.5, $\Delta v_{||} = 3\ v_t$ and $V_{||n} = v_r - 7\ v_t$ initially.

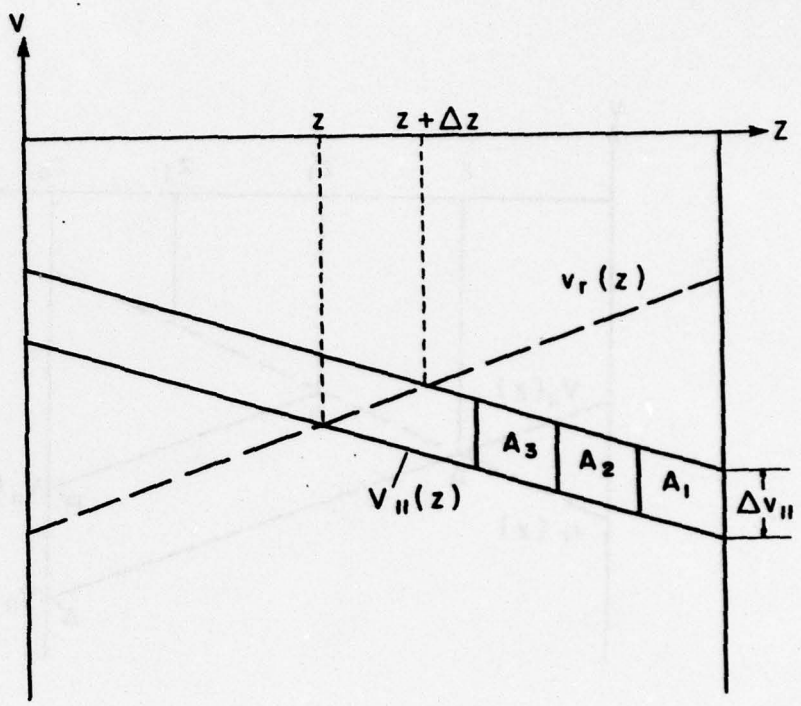

Figure 16. Schematic diagram of an equilibrium beam of electrons in the $v_{||}$ - z plane.

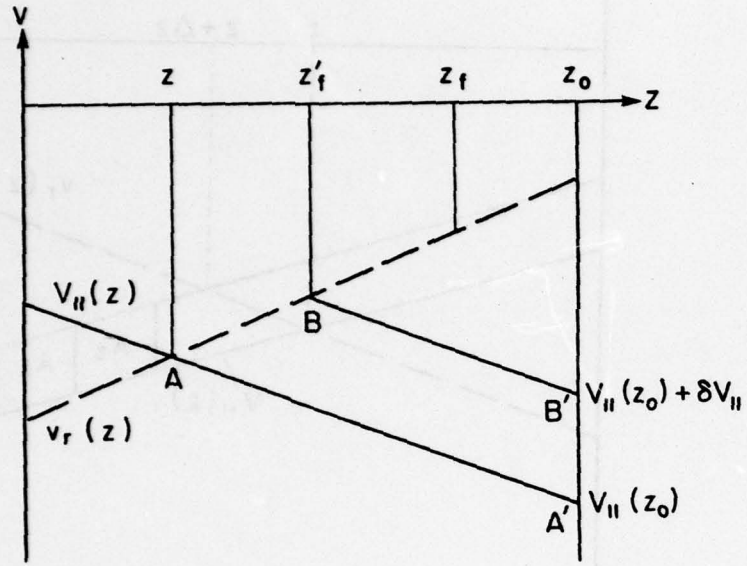

Figure 17. Distinction between untrapped and trapped electrons in the case of a wavepacket with an abrupt leading front.